ANALYSIS OF LOCAL MPPS ON THE P-V CURVE OF A PARTIALLY SHADED PV STRING

Georgios PSARROS(1) Efstratios BATZELIS(1) Stavros PAPATHANASSIOU(1)

(1) NTUA, Electric Power Division, 9 Iroon Politechniou str., 15780, Athens, Greece

e-mail: batzelis@mail.ntua.gr

ABSTRACT: In this paper, a comprehensive analysis on the local maxima developed in a partially shaded PV string, experiencing multiple irradiance levels, is presented. The number and the trends of the local and global maximum power points (MPPs) are studied, initially considering two irradiance levels and subsequently extending to the more complicated three-irradiance levels scenario. The shading patterns at which each MPP appears are investigated, and the conditions under which they constitute the global MPP (GMPP) are identified, while the effect of the operating temperature and the intensity of irradiance is studied.

Keywords: Global maximum power point (GMPP), maximum power point (MPP), multiple irradiance levels, partial shading, photovoltaic (PV) string, power peaks.

1 INTRODUCTION

When operating under partial shading conditions, the electrical response of a PV generator is significantly affected, giving rise to multiple maximum power points (MPPs). Previously published work on the performance of partially shaded PV systems deals with the appearance and characteristic trends of multiple MPPs [1]-[5]. In [1], two local MPPs are identified when a single PV module experiences two irradiance levels, while in [2] the general multi-irradiance case of a PV string is considered, leading to mathematical formulae for the evaluation of all potential local MPPs. Similarly, the partial shading phenomenon on PV arrays is studied in [6]-[10], while empirical expressions are proposed in [11] in order to quantify the voltage and current of the local MPPs appearing on the *I-V* and *P-V* curves of PV arrays.

Although these papers deal with the characterization and quantification of the potential MPPs, they do not shed light on the conditions for their appearance, since under some shading patterns certain MPPs appear while others do not. This is partially addressed graphically in [3]-[4] for the case of two irradiance levels, illustrating the relation of the number of MPPs to the extent and intensity of the shade. However, these papers consider only the number of MPPs and do not identify their type, nor do they study the global maximum (GMPP) trends.

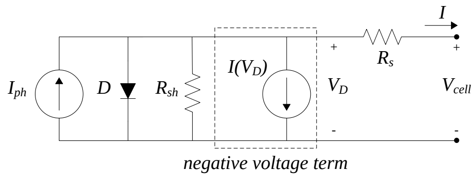

Figure 2: PV cell electrical equivalent circuit.

In this paper, a detailed analysis is carried out on the number of MPPs developed in a partially shaded PV string, the conditions for their appearance and the identification of the GMPP. The analysis extends beyond the two irradiance levels, while various operating irradiances and temperatures are considered.

The modeling of PV string adopted in this study is described in Section 2, while its operating principles under partial shading are discussed in Section 3. In Sections 4 and 5 the number of developed MPPs and the global maximum trends of a PV string illuminated by two and three irradiance levels, respectively, are classified for various shading patterns. The main conclusions are summarized in Section 6.

2 MODELING OF THE PV STRING

The PV string comprises several series connected PV modules, while a PV module consists of series connected PV cells. A group of series connected cells, with a bypass diode connected in parallel at its terminals, is denoted a cell string. The layout of a typical PV string is illustrated in Fig. 1.

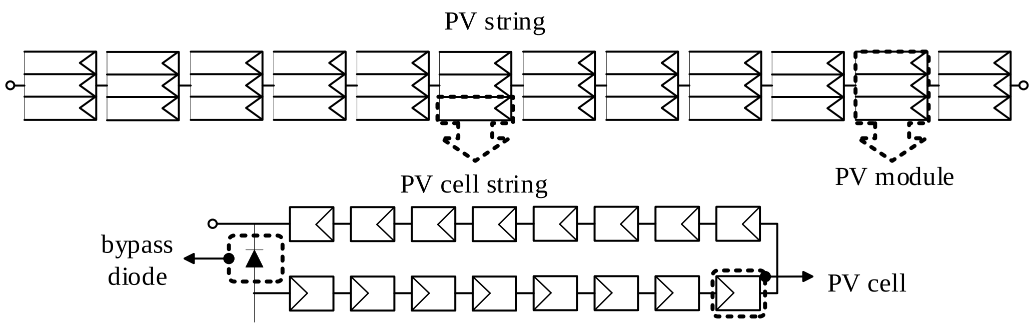

Figure 1: Layout of a PV string comprising 12 PV modules and its building components.

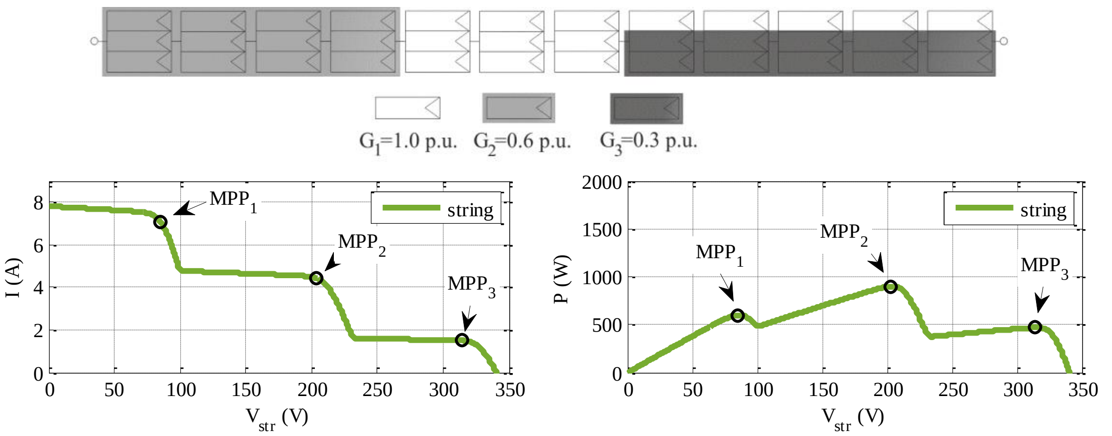

Figure 3: (a) *I-V* and (b) *P-V* curves of a PV string illuminated at 3 irradiance levels (G_1=1 p.u., G_2=0.6 p.u., G_3=0.3 p.u. /T_c=25°C).

In this study, in order to simulate the electrical response of the PV string, the single-diode PV cell electrical equivalent of Fig. 2 is adopted, properly enhanced for negative voltage operation [12]-[15]. Its operation is described by the following eq. (1), employing the Lambert *W* function to reduce computational complexity [2].

$$V_{cell}=\begin{cases} R_{sh}\left(I_{ph}+I_s\right)-\left(R_s+R_{sh}\right)\cdot I- \\ a\cdot W\left\{\dfrac{R_{sh}I_s}{a}e^{\frac{R_{sh}\left(I_{ph}+I_s-I\right)}{a}}\right\}, & I\le I_{ph} \\ V_{br}-I\cdot R_s-z_{R\min}, & I>I_{ph}\end{cases} \quad (1)$$

where I_{ph}, I_s, a, R_s and R_{sh} are the five parameters of the model, determined according to [16], b, V_{br}, m are coefficients related to negative voltage operation [12]-[14], $W\{x\}$ is the Lambert W function and $z_{R\min}$ the minimum real root of the following quartic function, as described in [2]:

$$\frac{1}{R_{sh}}\cdot z^4+\left(I_{ph}-I-\frac{V_{br}}{R_{sh}}\right)\cdot z^3+bV_{br}^3\cdot z-bV_{br}^4=0 \quad (2)$$

Eq. (3) gives the cell string voltage V_{cs} in an explicit manner, assuming a number of N_s cells connected in series.

$$V_{cs}=\begin{cases}\sum_{i=1}^{N_s}V_{cell-i}(I) & ,I\le I_{SC,cs} \\ -a_{bp}\cdot\ln\left(\dfrac{I-I_{SC,cs}}{I_{sbp}}+1\right) & ,I>I_{SC,cs}\end{cases} \quad (3)$$

Assuming that each PV module is composed by N_{cs} cell strings and each PV string comprises N_m modules, eq. (4) is used to calculate PV string voltage:

$$V_{str}=\sum_{i=1}^{N_m\cdot N_{cs}}V_{cs-i}(I) \quad (4)$$

3 PV STRING OPERATION UNDER PARTIAL SHADING CONDITIONS

Under partial shading conditions, a PV string may present no more than two local maxima, assuming two irradiance levels, denoted as MPP_1 and MPP_2 [1]-[2]. Extending to n irradiance levels, a PV string develops up to n local MPPs, denoted as MPP_1, MPP_2, ..., MPP_n [2].

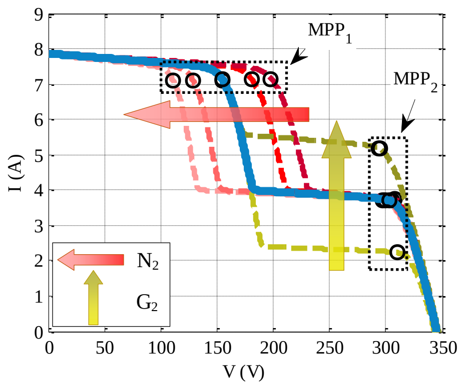

Figure 4: *I-V* curve of a PV string illuminated at two irradiance levels. The red and yellow arrows show how the characteristic is modified when the extent ($N_2/(N_1+N_2)$) or the intensity (G_2/G_1) of the shadow changes.

In Fig. 3, an indicative scenario of three irradiance levels G_1=1 p.u., G_2=0.6 p.u. and G_3=0.3 p.u. is illustrated, forming three groups of N_1=14, N_2=12 and N_3=10 cell strings illuminated at the respective irradiance levels. Three MPPs appear in this case, which are identified and classified as different MPP types according to [2]. At each MPP_j, the cell string groups 1 to j (assuming $G_i>G_j$, $i<j$) operate at the reduced current imposed by the irradiance level G_j, while the rest of the groups are shorted by their bypass diodes.

In particular, at MPP_1 only the group 1 (N_1=14) contributes to power generation, while groups 2 (N_2=12) and 3 (N_3=10) are bypassed. At MPP_2, cell string groups 1 and 2 operate at the current dictated by the irradiance level G_2 and group 3 is shorted, while at MPP_3 all cell string groups are forced to operate at the reduced current corresponding to irradiance level G_3, since no bypass diode conducts.

4 PARTIAL SHADING – 2 IRRADIANCE LEVELS

4.1 Number of MPPs

A PV string illuminated at two different irradiance levels may present one or two

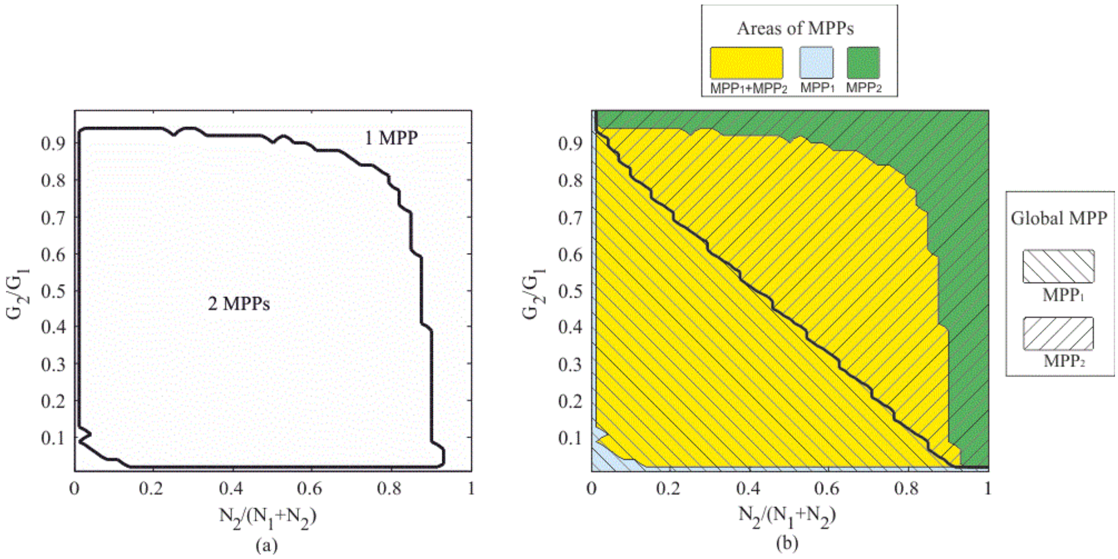

Figure 5: (a) Number and (b) classification of the MPPs versus the extent ($N_2/(N_1+N_2)$) and intensity (G_2/G_1) of the shadow, for a PV string illuminated at two irradiance levels.

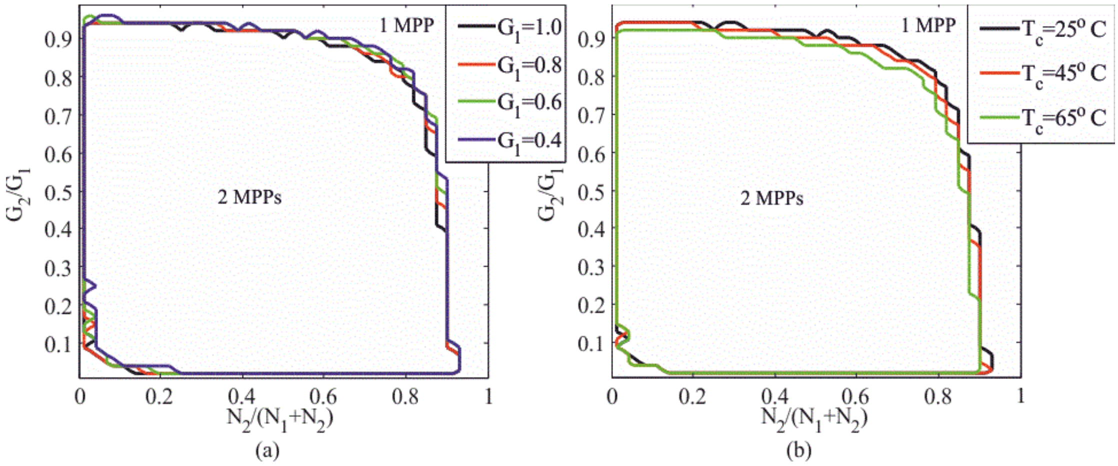

Figure 6: Number of MPPs for (a) varying irradiance on the unshaded cell strings G_1 (T_c=25° C) and (b) varying operating temperature T_c (G_1 =1.0 p.u.).

MPPs, according to the shading pattern and intensity. In Fig. 4, the electrical response of the PV string of Fig. 1 is depicted in blue, for an indicative shading scenario (G_1=1 p.u., G_2=0.5 p.u., N_1=22, N_2=14), developing two local MPPs (MPP_1 and MPP_2). This shading pattern is subsequently varied to cover all possible cases, changing its extent ($N_2/(N_1+N_2)$) from fully shaded to unshaded and its relative intensity (G_2/G_1) from 0.01 to 1 (G_1=1 p.u. and operating temperature T_c=25°). Variation of the shade extent shifts MPP_1 horizontally (red dashed *I-V* curves of Fig. 4), while the shade intensity shifts MPP_2 vertically (yellow dashed *I-V* curves of Fig. 4), as indicated by arrows in Fig. 4.

This trend is displayed in Fig. 5. In Fig. 5(a), the number of MPPs developing on the *I-V* characteristic is depicted on the plane of the extent and intensity of shade. A single MPP will arise only at the boundary area, where the string experiences a shade either too deep or too extended.

The characterization of the MPPs as MPP_1 or MPP_2, defined above, is shown in Fig. 5(b). Three areas are presented: the two-MPP area, where both MPP_1 and MPP_2 appear, is colored in yellow; the single MPP area is split into sub-regions where the MPP is either an MPP_1 (light blue) or MPP_2 (green). Hatching indicates whether the MPP_1 or the MPP_2 is the global MPP.

A detailed observation of Fig. 5 leads to the conclusion that when G_2 is higher than 95% of G_1 or the number of shaded cell strings (N_2) exceeds the 95% of the total number (N_1+N_2), only MPP_2 is developed on the *P-V* curve of the string. On the other hand, the single MPP is MPP_1 only when the number of shaded cell strings (N_2) is less than 2% of the string or at unrealistically heavy shade levels. Consequently, a single MPP appears at boundary shading scenarios, where the shaded area is very high (>95% - MPP_2) or too small (<2% - MPP_1), or the depth of shade is negligible (>95% - MPP_2). In the two-MPP region, the global maximum GMPP may be MPP_1 or MPP_2, depending on the shading pattern, as shown in Fig. 5(b).

4.2 Various operating irradiance and temperature

This analysis is extended in Fig. 6 for cases that the irradiance on the unshaded part G_1 and the operating temperature T_c deviate from STC. As shown in Fig. 6(a), the absolute value of G_1 does not

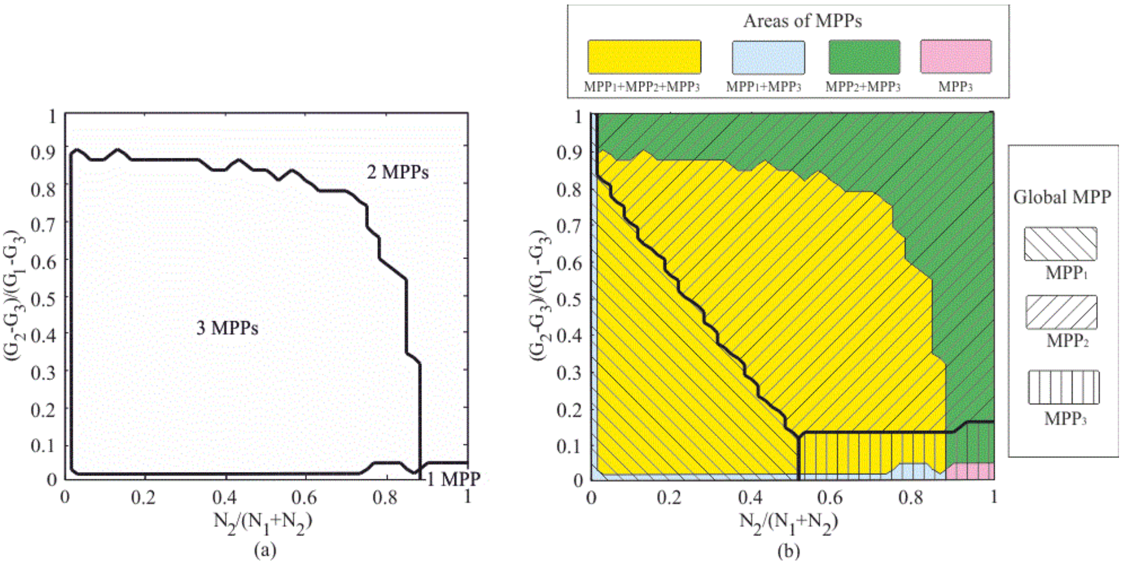

Figure 7: (a) Number and (b) classification of the MPPs versus the extent ($N_2/(N_1+N_2)$) and intensity ($(G_2-G_3)/(G_1-G_3)$) of the shadow, for the PV string of Fig. 1, illuminated at three irradiance levels and assuming G_3/G_1=0.3 and N_3=6.

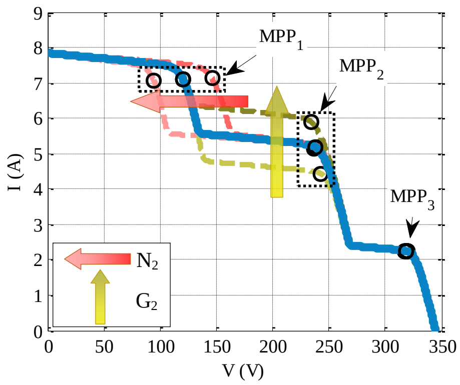

Figure 8: *I-V* curve of a PV string illuminated at three irradiance levels, assuming N_3 and G_3 are constant. Red and yellow arrows show how the characteristic is affected when the extent ($N_2/(N_1+N_2)$) or the relative intensity ($(G_2-G_3)/(G_1-G_3)$) of the shadow change.

have any notable effect, because the MPPs depend only on the relative shade intensity G_2/G_1. In Fig.6(b) the two-MPP region shrinks slightly at high cell temperatures, yet this effect is again not significant. As similar observations hold also for the relative importance of MPP_1 and MPP_2 in forming the global MPP (GMPP), it can be concluded that in the general case of a partially shaded PV string, MPPs are determined by the relative shade intensity and extent, rather than by the absolute irradiance values or the temperature.

5 PARTIAL SHADING – 3 IRRADIANCE LEVELS

5.1 Constant N_3 and G_3

In order to extend the analysis to the general multi-irradiance case, the indicative scenario of three irradiance levels G_1=1.0 p.u., G_2=0.7 p.u., G_3=0.3 p.u., with N_1=18, N_2=12 and N_3=6, is examined in Fig. 8. The horizontal red double arrow implies the relative variation of the lightly shaded cell strings N_2 with respect to the sum N_1+N_2. The number N_3 of heavily shaded cell strings is considered constant. The vertical yellow double arrow indicates variation of G_2 in the range from G_3 to G_1, assuming again that G_1 and G_3 are constant.

In this case, the relevant parameters are the relative shade intensity $(G_2-G_3)/(G_1-G_3)$ on the lightly shaded part of the string, comprising N_2 cell strings, and the relative extent $N_2/(N_1+N_2)$ of the lightly shaded part of the string. The parameters G_3, G_1 and N_3 are initially considered constant. In Fig. 7(a), the number of MPPs is illustrated assuming N_3=6 cell strings, G_1=1.0 and G_3=0.3.

Apparently, a number of up to three MPPs may arise depending to the shading pattern. Typically, 3 MPPs are presented, whereas one or two MPPs appear only at the boundary areas of Fig. 7(a). To further understand which MPP is presented and which one is suppressed in each case, the categorization in the MPP_1, MPP_2 and MPP_3 types is shown in different color in Fig. 7(b). In the central yellow colored region all three MPPs appear, while the green and light blue areas correspond to two local maxima (MPP_2+MPP_3 and MPP_1+MPP_3 respectively). The single MPP case appears only when the shading intensities are almost equal ($G_2 \approx G_3$) and the unshaded part of the string is very limited ($N_2/(N_1+N_2) \geq 0.9$). In this case, the single MPP is of the MPP_3 type. It is evident that MPP_3 is present in all cases because of the minimum heavy shade extent of N_3=6 cell strings considered in all examined patterns. Despite the small extent of the latter, it is notable that the MPP_1 and MPP_2 are never presented as the single MPP of the string, nor does the combination MPP_1+MPP_2 ever appear as a two-MPP case. The hatching patterns in Fig. 7(b) indicate which MPP type (MPP_1, MPP_2 or MPP_3) is the global one in each case, MPP_2 being the most common case.

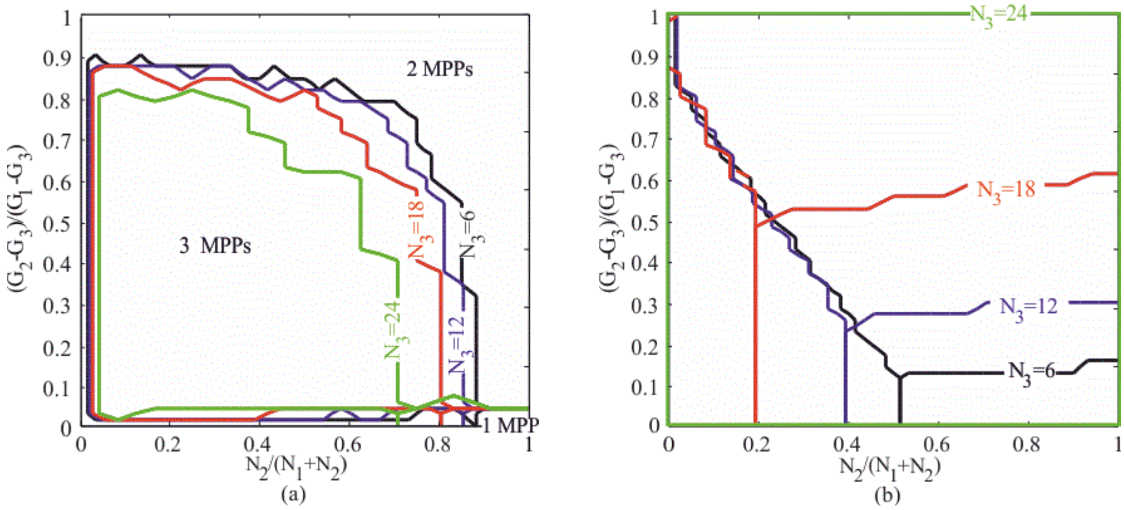

Figure 9: (a) Number of MPPs and (b) global maximum for a PV string illuminated at three irradiance levels, for a varying number N_3 of heavily shaded cell strings (G_3/G_1=0.3).

5.2 Impact of N_3 variation

In the scenarios studied above, the heavy shade extent has been considered constant (N_3=6 cell strings) for illustration purposes. In the following, N_3 is varied in the range 6 to 24 out of 36 total cell strings. The effect on the I-V characteristic is shown with the green arrow in Fig. 10.

The number of MPPs is shown in Fig. 9(a), where the central three-MPP region seems to shrink with the increment of N_3, leaving more space to the two-MPP area and specifically to the MPP_2+MPP_3 region. This is reasonable, since the unshaded and lightly shaded areas are reduced in these cases, leading to weakening of MPP_1 and MPP_2, unlike MPP_3 which is strengthened. This is clear in Fig. 9(b), in which the global maximum origination is depicted. As N_3 increases, the MPP_3 is more often the GMPP, until it becomes always the global maximum for N_3=24 cell strings and beyond.

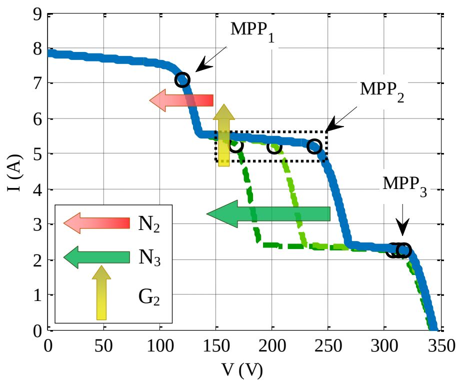

Figure 10: *I-V* curve of a PV string illuminated at three irradiance levels (assuming that G_3 is constant). Red, yellow and green arrows show how the characteristic is modified when the extent ($N_2/(N_1+N_2)$) and the intensity ((G_2-G_3)/(G_1-G_3)) of the light shadow or the number of heavily shaded cell strings N_3 change.

5.3 Impact of G_3 variation

The impact of the deep shadow irradiance level G_3 on the *I-V* curve of the PV string is shown in Fig. 11 (brown arrow), considering now its extent to be constant (N_3=6 cell strings).

In Fig. 12(a), the number of MPPs is examined for four different values of G_3. The central three-MPP region appears to shrink with the increment of G_3, as in Fig. 9(a), giving space to the MPP_2+MPP_3 region. At the same time, MPP_3 is the GMPP more often, as depicted in Fig. 12(b), while for G_3=0.8 it becomes the global MPP in all cases.

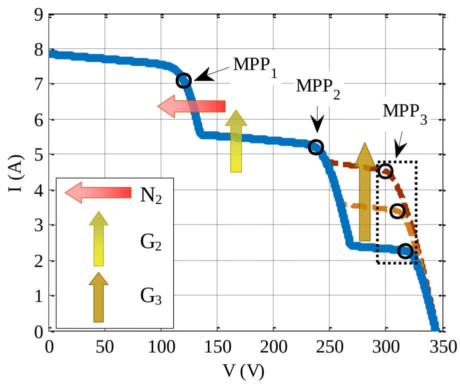

Figure 11: *I-V* curve of a PV string illuminated at three irradiance levels, assuming a constant N_3. Red and yellow arrows show how the characteristic is modified when the relative extent ($N_2/(N_1+N_2)$) and intensity ((G_2-G_3)/(G_1-G_3)) of the light shadow changes. The brown arrow presents the effect of irradiance G_3 variations.

6 CONCLUSION

In this paper, the number and type of the local MPPs, as well as the global maximum origination, are analyzed for a PV string illuminated at multiple irradiance levels.

For two irradiance levels, it is concluded that two MPPs (MPP_1 and MPP_2) usually appear and they share equally the probability to act as the GMPP, MPP_2 being the global maximum under light shadow or limited shade extent conditions. Furthermore, it isobserved that the absolute

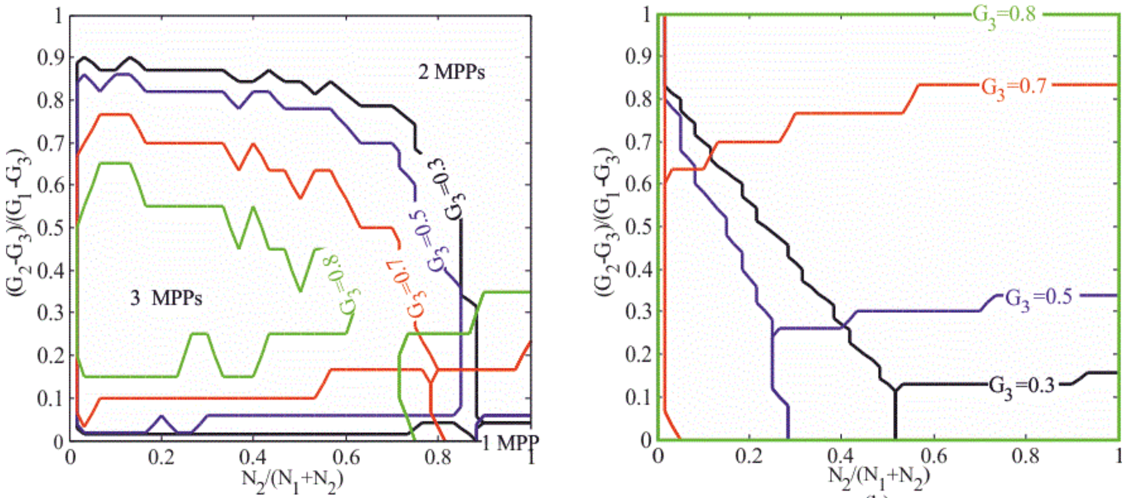

(a) (b)

Figure 12: (a) Number of MPPs and (b) global maximum of a PV string illuminated at three irradiance levels, for varying deep shadow irradiance level G_3 ($N_{3=}6$).

irradiance levels (G_1, G_2) and the operating temperature do not affect the correlation of the MPPs.

For three irradiance levels on the string, it is observed that in most cases all three MPPs (MPP_1, MPP_2 and MPP_3) appear, but the global MPP in each case is determined by the extent and intensity of the light and heavy shadows. The gradual increment of the heavy shadow extent (N_3) or its corresponding irradiance (G_3) leads to the rightmost MPP (MPP_3) becoming more frequently the global maximum.

7 ACKNOWLEDGMENTS

The work of Mr. G. Psarros was supported by the State Scholarships Foundation (IKY). Mr. E. Batzelis is supported in his PhD studies by "IKY Fellowships of Excellence for Postgraduate Studies in Greece - Siemens Program".

8 REFERENCES

[1] E. Paraskevadaki, and S. Papathanassiou, “Evaluation of MPP voltage and power of mc-Si PV modules in partial shading conditions,” *IEEE Trans. Energy Covers.*, vol. 26, no. 3, pp. 923–932, Sep. 2011.

[2] E. Batzelis, I. Routsolias, and S. Papathanassiou, “An explicit PV string model based on the Lambert W function and simplified MPP expressions for operation under partial shading,” *IEEE Trans. Sust. Energy*, vol. 5, no. 1, pp. 301–312, Jan. 2014.

[3] Maki, S. Valkealahti, and J. Leppaaho, “Operation of series-connected silicon-based photovoltaic modules under partial shading conditions,” *Prog. Photovolt.: Res. Appl.*, vol. 20, no.3, pp. 298-309, 2012.

[4] A. Maki, and S. Valkealahti, “Effect of photovoltaic generator components on the number of MPPs under partial shading conditions,” IEEE Trans. Energy Conv., vol. 28, no.4, pp. 1008-1017, Dec. 2013.

[5] A. Maki, and S. Valkealahti, “Power losses in long string and parallel-connected short strings of series-connected silicon-based photovoltaic modules due to partial shading conditions,” *IEEE Trans. Energy Conv.*, vol. 27, no.1, pp. 173-183, 2012.

[6] F. Martinez-Moreno, J. Munoz, and E. Lorenzo, “Experimental model to estimate shading losses on PV arrays,” *Sol. Energy Mater. Sol. Cells*, vol. 94, no.12, pp. 2298–2303, Dec. 2010.

[7] N. Thakkar, D. Cormode, V. Lonij, S. Pulver, and A. Cronin, “A simple non-linear model for the effect of partial shade on PV systems,” in *Proc. 35th PVSC 2010*, Honolulu, HI, United States, Jun. 2010, pp. 2321–2326.

[8] P. Rodrigo, E. F. Fernández, F. Almonacid, and P.J. Pérez-Higueras, “A simple accurate model for the calculation of shading power losses in photovoltaic generators,” *Sol. Energy*, vol. 93, pp. 322-333, Jul. 2013.

[9] K. Brecl and M. Topic, “Self-shading losses of fixed free-standing PV arrays,” *Renew. Energ.*, vol. 36, no. 11, pp. 3211-3216, Nov. 2011.

[10] C. Deline, A. Dobos, S. Janzou, J. Meydbray, and M. Donovan, “A simplified model of uniform shading in large photovoltaic arrays,” *Sol. Energy*, vol. 96, pp. 274-282, Oct. 2013.

[11] S. Moballegh and J. Jiang, “Modeling, prediction, and experimental validations of power peaks of PV arrays under partial shading conditions,” *IEEE Trans. Energy Convers.*, vol. 5, no. 1, pp. 293-300, Jan. 2014.

[12] S. Silvestre and A. Chouder, “Effects of shadowing on photovoltaic module performance,” *Prog. Photovolt.: Res. Appl.*, vol. 16, no.2, pp. 141-149, Mar. 2008.

[13] M.F.N. Tajuddin, S.M. Ayob, and Z. Salam, “Tracking of maximum power point in partial shading condition using differential evolution (DE),” in *Proc. PECon 2012*, Kota Kinabalu, Malaysia, Dec. 2012, pp. 384-389.

[14] H. Kawamura, K. Naka, N. Yonekura, S. Yamanaka, H. Kawamura, H. Ohno, and K. Naito, “Simulation of characteristics of a PV

module with shaded PV cells," *Sol. Energy Mater. Sol. Cells*, vol. 75, no.3-4, pp. 613–621, Feb. 2003.

[15] J. W. Bishop, "Computer simulation of the effects of electrical mismatches in photovoltaic cell interconnection circuits," *Sol. Cells*, vol. 25, no.1, pp. 73–89, 1988.

[16] W. De Soto, S.A. Klein, and W.A. Beckman, "Improvement and validation of a model for photovoltaic array performance," *Sol. Energy*, vol. 80, no.1, pp. 78-88, Jan. 2006